



Aspects of kinetic modeling of fixed bed reactors

Yves Schuurman*

IRCELYON, UMR5256 CNRS Université Lyon 1, 2 Avenue Albert Einstein, 69626 Villeurbanne, France

ARTICLE INFO

Article history:

Available online 11 June 2008

Keywords:

Kinetics
Transport limitations
Structured reactors
Partial oxidation of methane

ABSTRACT

This paper briefly reviews the most important aspects of catalyst testing in packed-bed catalytic laboratory reactors to properly assess the intrinsic chemical kinetics. Next it discusses approaches to assess the kinetics of fast reactions or those accompanied with strong heat effects that cannot be performed in a packed-bed reactor configuration free from transport limitations. As an example the partial oxidation of methane is presented in a steady-state fixed bed reactor as well as in a TAP (temporal analysis of products) reactor. The continuing increase in computational power leads to more sophisticated reaction and reactor models due to the increasing use of computational chemistry and computational fluid dynamics in reaction engineering.

© 2008 Elsevier B.V. All rights reserved.

1. Introduction

The scale-up of reactions carried out at the level of the laboratory to an industrial unit constitutes the traditional discipline of chemical engineers. It has been evolving ever since by responding to the societal needs and developments. Wintermantel [1] divides process scale-up into two parts: the 'scientific part' consist in analyzing complex systems in terms of subsystems that are described using our understanding of fundamental chemical and physical processes. The 'engineering part' consists in using this knowledge in the design and construction of a working plant despite the fact that our understanding is still incomplete. The ever-tighter economic, environmental, safety and social pressures require more and more optimal process designs. This means more sophisticated models based on physical processes rather than on empirical relations. This has led to multiscale approaches [2,3], which replaces the conventional sequential mode of scale-up into a highly parallel one.

Catalytic reactors are at the heart of the majority of chemical processes. Inside the catalytic reactor multiple chemical and physical processes take place at different length and time scales and often in different phases. The proper design of a catalytic reactor requires the knowledge of the rate of reaction and the selectivity as a function of the operating conditions. Preferably a rate expression based on the *intrinsic* reaction kinetics is used to translate laboratory data to pilot scale and further to an industrial unit. Without reliable kinetics, the reactor design is rather

speculative and it is not really possible to evaluate the deviations and the dynamics that occur in the reactor. This constitutes a critical step in assessing the operational safety and environmental impact of the production unit [4].

The computational power available today allows using more and more sophisticated mathematical models and thus faster and better process design. Computational methods take a more and more prominent role in reactor modeling. On one hand, theoretical chemistry allows mechanistic ideas to be pursued and the prediction of physical and thermodynamical properties of reactants and products [5,6]. On the other side of the spectrum computational fluid dynamics (CFD) are used to get an understanding of the role of the hydrodynamics and the heat transfer on the overall reactor performance [7]. Experimental methods for kinetics and heat and mass transfer measurements have also strongly evolved over the last decade.

Catalytic fixed bed reactors are the main reactor type used for large-scale heterogeneously catalyzed gas-phase reactions. They are also often the reactor of choice in the laboratory for kinetic studies.

This paper will focus on the above aspects of modeling of fixed bed catalytic reactors as well as on the acquisition of the experimental data, and will give examples of the different approaches. The basic principles and details on reactor modeling can be found in classical textbooks [8,9].

2. Kinetics in fixed bed reactors

The design of an industrial reactor can only be done reliably if it is based on intrinsic kinetic data. Apparent kinetics, kinetics based on pellet scale, can only be used if a similar reactor is scaled-up

* Tel.: +33 472445482; fax: +33 472445399.

E-mail address: yves.schuurman@ircelyon.univ-lyon1.fr.

with the same catalyst size and geometry and in the absence of thermal effects.

In order to measure in a packed-bed reactor properly the kinetics, either intrinsic or apparent, the hydrodynamics need to be known and well defined. Uniform flow velocities, known as plug flow, or parabolic flow velocities such as in structured reactors are preferred.

The behavior of the flow through a packed-bed depends on the Reynolds number (Re). Re numbers for packed-bed reactors are based on the average particle size and the interstitial or pore velocity. Dixon et al. [7], reviewed the results on the flow regimes obtained in packed-beds from different experimental studies and presented four flow regimes, proposed originally by Dwybbs and Edwards [10], for different ranges of Reynolds numbers:

1. " $Re < 1$: Viscous or creeping flow in which pressure drop is linearly proportional to interstitial velocity and flow is dominated by viscous forces;
2. $10 < Re < 150$: Steady laminar inertial flow in which pressure drop depends nonlinearly on interstitial velocity and boundary layers in the pores become pronounced with an "inertial core" appearing in the pores;
3. $150 < Re < 300$: Unsteady laminar inertial flow in which laminar wake oscillations appear in the pores and vortices form at around $Re = 250$;
4. $Re > 300$: Highly unsteady flow, chaotic and qualitatively resembling turbulent flow."

In lab scale reactors Re numbers are well below 150, often the values are below 10. The presence of the particles smoothes out the laminar velocity profile and a uniform profile is obtained in a fixed bed reactor if the wall effects and axial dispersion are negligible. Due to the flat wall the catalyst bed porosity in the vicinity of the reactor wall is higher than in the rest of the bed giving higher flow velocities close to the wall. This effect can be neglected by choosing a ratio of the reactor diameter to the particle diameter larger than 10. Similarly, the axial dispersion can be neglected by choosing a ratio of the reactor length to the particle diameter larger than 50. A more precise criterion is available that takes the conversion into account [11].

When a fluid is brought into contact with a solid catalyst on which a chemical reaction occurs, various physical and chemical processes take place on different time and length scales. Fig. 1 schematizes some of these processes. For example, heat generated at the catalytic site is transported by conduction through the pellet to the fluid phase. At the level of the catalyst bed the heat is conducted in both the radial and axial direction. The fluid transports the heat by convection and conduction in the axial direction and by conduction in the radial direction. At the vicinity of the wall, heat is conducted through a stagnant fluid film and then through the wall to the coolant fluid on the shell side. Current heat transfer models for packed-beds lump several heat transfer mechanisms into an effective parameter, because many of the physical processes are too complex and involve too many parameters or are not yet understood well enough on a fundamental level. Similar processes take place on the different time and length scales for mass transport. A mathematical model for a reactor design needs to take into account all these processes, but a model to extract kinetic parameters from experimental data will be too sophisticated and will be computationally too expensive. Moreover, if transport limitations occur during kinetic experiments this will lead to a large uncertainty on the kinetic parameters. Thus to measure the intrinsic kinetics the reactor configuration and the operating conditions need to be chosen such that all transport limitations can be neglected compared to the rate of the chemical reaction. In order to assess the influence of transport limitations, criteria have been derived that evaluate a $\pm 5\%$ deviation of the intrinsic rate [12,13]. Kapteijn and Moulijn discuss extensively the different criteria and their usage [11]. The same criteria are used to estimate the transport processes that will occur in the industrial reactor and permit the right choice of reactor model.

These criteria contain many transport parameters that need to be known. They are estimated from various correlations that are valid for certain operating conditions. Using different correlations can lead to significantly different results and the correlations should be carefully chosen for both the experimental reactor and the industrial unit to be designed. There is still a need for adequate correlations for mass and heat transfer at low Re numbers, conditions used in the laboratory.

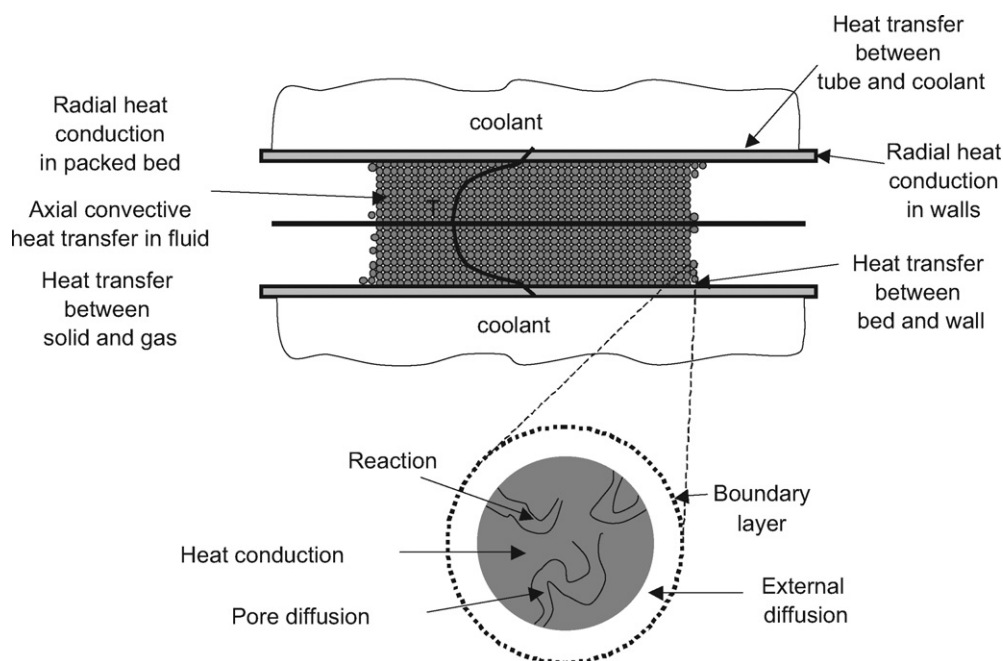


Fig. 1. Illustration of different transport phenomena on different scales in a packed-bed reactor.

Diagnostic experimental tests exist but they are not always very conclusive due to the possible existence of other simultaneous transport limitations [11].

3. Irreducible transport phenomena

There are limits to which the reactor and catalyst dimensions in a packed-bed configuration can be reduced before other limitations may occur. Reducing the catalyst particle diameter or the reactor diameter will lead to increased pressure drop. For very fast reactions, often accompanied with strong heat effects, no operating conditions in a fixed bed reactor might be feasible that allow to operate in the kinetic regime. In that case the transport process has to be taken into account explicitly by the use of a heterogeneous model. In recent years, reactors have been developed that are aimed at minimizing transport limitations or that employ well-defined hydrodynamics that can be easily accounted for in a reactor model.

Reactors such as microstructured devices, annular or coated wall reactors and monoliths have the following advantages: thin layers of catalysts to reduce internal diffusion limitation, structured materials to obtain a low pressure drop, small dimensions for fast transport and often good heat conducting materials for good temperature control. On lab scale these reactors operate in the laminar flow regime and the radial mixing is less than in fixed bed reactors. Different criteria than those for fixed bed reactors are needed for these reactor configurations and different correlations for mass and heat transfer coefficients are necessary. For example, the external mass transfer coefficient in coated wall reactors is independent of the flow rate.

Laminar flow through circular ducts requires a two-dimensional flow model to describe the velocity and concentration field accurately in both radial and axial direction. For kinetic studies involving parameter estimation simplified models are preferred. Different one-dimensional approaches have been proposed. Commenge et al. [14] compared a two-dimensional convection–diffusion equation for transport and reaction in cylindrical channels with a first-order reaction at the wall to a pseudo-homogeneous plug-flow model and a one-dimensional dispersion model. They have solved the 2D problem numerically and have compared the results to the two 1D solutions. In this way they were able to examine the influence of radial mass transfer on the accuracy of heterogeneous kinetic measurements in micro-channel reactors. The error induced on the heterogeneous rate constant measurement by using the plug-flow assumptions depends strongly on the value of the Damköhler number. For Damköhler numbers smaller than 0.1 the error in the rate constant is less than 3%.

Berger and Kapteijn [15] have developed criteria involving only the observed conversion to justify the absence of radial concentration gradients and to be able to use the simple plug-flow model to describe the reactor performance.

The benefit of thin catalyst layers has been demonstrated for the water–gas shift reaction over a Pt/CeO₂/Al₂O₃ catalyst [16]. The conversion of CO was measured as a function of temperature over a powder sample with an average particle size of 250 µm and over the same catalyst prepared by a sol–gel method in stainless steel micro-channels. The equivalent particle diameter of the catalyst layer inside the micro-channel was 37 µm. The initial rates at low temperatures are similar for both geometries. However, the conversion at higher temperatures over the powder samples is lower than that of platelets indicating diffusion limitation inside the powder grains. A simulation taking into account the diffusion of the reactants and products inside the catalyst pores confirmed

this. This kinetic study was extended and a detailed mechanism for the water–gas shift reaction over a Pt/CeO₂/Al₂O₃ catalyst was derived [17].

Other microstructured devices [18–20], annular [21,22] or coated wall reactors [23] have been used for kinetic studies. Other structured catalyst configurations have also been used such as foams and fibers [24–26].

The TAP (temporal analysis of products) reactor is another device well adapted for both mechanistic and kinetic studies of fast reactions. The low pressures and small pulse quantities applied in the TAP reactor lead to a number of conditions that are quite different from those encountered in fixed bed experiments. The pressure in the reactor is on the order of 20–200 Pa and the ratio of reactant molecules to number of active sites is on the order of 0.01 thus implying very low surface coverages [27,28]. These conditions, although quite different than those used in industrial catalytic reactors, lead to advantages that allow the study of processes not easily feasible by other (transient) methods. The low pressures applied in the TAP reactor lead to transport through the packed-bed by Knudsen flow thus excluding all gas-phase reactions. This mode of transport also excludes any external mass transfer limitations, as diffusion is the only mode of transport. The time resolution of TAP experiments is on the order of sub millisecond, about two orders of magnitude better than flow experiments, thus allowing the study of very fast reactions. A good isothermal reactor operation is possible as heat effects are negligible due to the use of small amounts of reactants. The TAP reactor has been successfully used to study high temperature processes such as methane oxidation, dry reforming, ammonia oxidation and HCN synthesis [29–34].

The following section compares two studies on the oxidation of methane in a steady-state fixed bed reactor [35,36] as well as in a TAP reactor [31]. In both cases a platinum gauze is used as a catalyst. The reactor models in the two studies take explicitly the relevant transport phenomena into account.

4. Partial oxidation of methane

At present, synthesis gas is produced mainly by endothermic steam-reforming, over a Ni-based catalyst [37]. The catalytic partial oxidation of methane with oxygen to synthesis gas, which is thermodynamically favored at high temperatures, has received attention as an alternative to steam-reforming.

This reaction runs at temperatures above 900 °C over Pt, Rh or Pt/Rh at very short contact times to avoid further oxidation of the syngas into carbon dioxide and water. Qualitative TAP experiments showed that CO and H₂ are indeed primary products [30,31]. de Smet et al. [35,36] studied the partial oxidation of methane in a continuous flow reactor set-up over a single wire Pt gauze. The gases were pre-heated before reaching the catalyst. A Pt-10%Rh thermocouple was attached to the Pt gauze to measure the surface temperature. Two thermocouples were located upstream and downstream of the gauze to measure the gas-phase temperature. The average bulk gas temperature was found to be 200 K lower than the catalyst surface temperature due to heat transfer limitations. de Smet et al. observed a constant methane conversion of 5% and a constant oxygen conversion of 18% at temperatures between 1025 K and 1225 K, indicating that the reaction rates are strongly influenced by transport limitations. In the same temperature range the CO selectivity increased linearly with the temperature from 20% to 53%. The CO selectivity decreased with increasing contact times at 1123 K. No hydrogen was formed, only the formation of water was observed. Similar trends were observed in other studies [38–42]. de Smet et al. calculated the gas-phase temperature and the mole fraction

Table 1
Reaction mechanism used by de Smet et al. [36]

No.	Reaction	A or s^0 ($\text{Pa}^{-1} \text{s}^{-1}$ or s^{-1})	E_{act} (kJ mol $^{-1}$)
1	$\text{O}_{2,\text{g}} + 2^* \rightarrow 2\text{O}^*$	0.023	0
2	$\text{CH}_4 + 2\text{O}^* \rightarrow \text{C}^* + 2\text{H}_2\text{O}_{\text{g}} + ^*$	2.4×10^5	48.2
3	$\text{C}^* + \text{O}^* \rightarrow \text{CO}^* + ^*$	1×10^{13}	62.8
4	$\text{CO}^* + \text{O}^* \rightarrow \text{CO}_{2,\text{g}} + 2^*$	1×10^{13}	100
5a	$\text{CO}^* \rightarrow \text{CO}_{\text{g}} + ^*$	1×10^{13}	126
5b	$\text{CO}_{\text{g}} + ^* \rightarrow \text{CO}^*$	0.84	0

profiles in case of a model surface reaction taking into account the 3D geometry of the gauze using the FLUENT CFD software. The measured surface temperatures were imposed at the wire surface in the calculations. The model surface reaction was represented by the following equation:

$$r_{\text{CH}_4} = k' C_{\text{CH}_4}^n$$

The 3D model is computationally too expensive and moreover, the FLUENT package did not allow more complex kinetics thus this approach is not suited for a kinetic study. In fact the authors used the FLUENT simulations to validate a simplified model that can account for detailed kinetics. Two major simplifications were introduced that reduced the CPU time by four orders of magnitude: The 3D gauze catalyst was replaced by two rows of flat plates (2D) and heat and mass transfer coefficients were obtained from the Nu and Pr equations for forced convection of gases to a cylinder in crossflow [43]. A five-step reaction model was used to describe the experimental data, reproduced in Table 1.

All reaction steps were considered irreversible, except the sorption step (5) of carbon monoxide. The pre-exponential factor and the apparent activation energy for the methane activation step were estimated by a regression analysis of the experimental CO selectivities. Note that the methane activation step is oxygen

assisted to explain the decreasing CO selectivity with increasing space-time. All the kinetic parameters of the other four steps were fixed at values obtained from the literature. The above reaction model gave an adequate description of the experimental data.

Another approach to model the kinetics of the partial oxidation of methane was by TAP experiments [31,41]. A high temperature TAP reactor was developed that operates at 1000 °C. Fig. 2 shows a schematic of the reactor and the axial temperature profile. Due to the water-cooling of the viton o-rings, the inlet and outlet of the reactor are at much lower temperatures. A single Pt gauze of 14 mm in diameter was used as a catalyst. Prior to its use the Pt gauze was oxidized by a series of pulses or a continuous flow of oxygen at 900 °C. This pretreatment corresponded to an oxygen uptake by the platinum of 200 and 26,000 monolayers, respectively. Thus a large reservoir of sub-surface oxygen exists. Oxygen and methane were pulsed over the oxidized platinum by varying the time interval between oxygen and methane. Both the selectivity to carbon monoxide and hydrogen increased with increasing separation between the oxygen and methane pulses while the methane conversion dropped slightly. This is due to a decrease of the concentration of surface oxygen with increasing pulse interval thus preventing the consecutive oxidation of carbon monoxide and hydrogen, resulting in very high selectivities. The product distribution is completely determined by the surface oxygen concentration. At high surface oxygen concentrations the consecutive reactions of carbon monoxide and hydrogen are much faster than the corresponding desorption steps. However, at low surface oxygen concentrations the diffusion of bulk oxygen is slow compared to the residence time of carbon monoxide and hydrogen and negligible complete oxidation occurs. The surface lifetime of carbon is much longer and the diffusion of oxygen becomes then rate determining for the formation of carbon monoxide. The pulse responses of the reactants and products at 800 °C and 950 °C are shown in Fig. 3. The methane and oxygen conversions increase

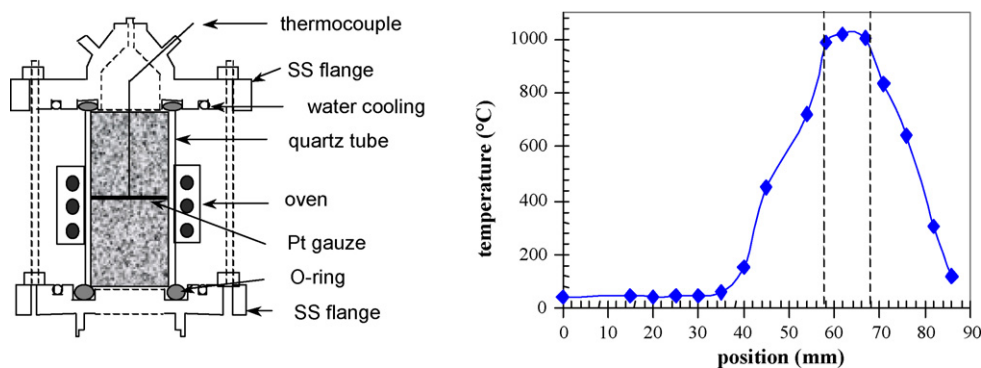


Fig. 2. High temperature TAP quartz reactor (left) and the temperature profile for a set-point of 1000 °C.

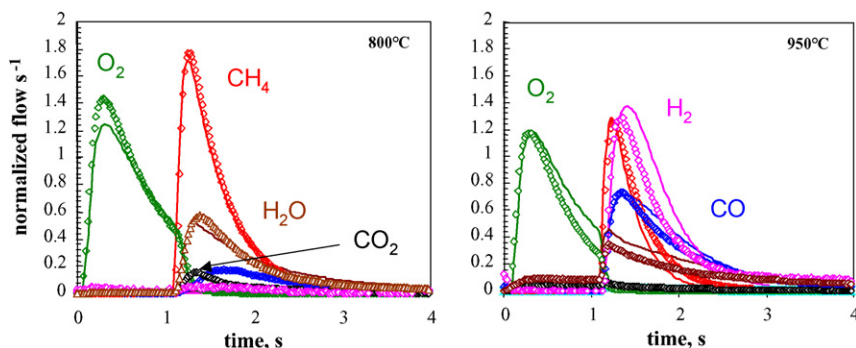


Fig. 3. TAP pulse responses of oxygen followed after 1 sec by methane over a pre-oxidized Pt gauze at 800 °C and 950 °C.

Table 2

Reaction mechanism used to model TAP pulse response data

No.	Reaction	Forward		Back	
		A or s^0 ($\text{Pa}^{-1} \text{s}^{-1}$ or s^{-1})	E_{act} (kJ mol^{-1})	A or s^0 ($\text{Pa}^{-1} \text{s}^{-1}$ or s^{-1})	E_{act} (kJ mol^{-1})
1	$\text{CH}_4 + 5\text{Pt}_\text{s} \rightleftharpoons \text{Pt}_\text{s}\text{C}_\text{s} + 4\text{Pt}_\text{s}\text{H}_\text{s}$	4.4×10^8	134	–	–
2	$\text{O}_2 + 2\text{Pt}_\text{s} \rightleftharpoons 2\text{Pt}_\text{s}\text{O}_\text{s}$	0.007	0	5×10^{12}	162
3	$\text{CO} + \text{Pt}_\text{s} \rightleftharpoons \text{Pt}_\text{s}\text{CO}_\text{s}$	0.02	0	1×10^{13}	126
4	$\text{CO}_2 + \text{Pt}_\text{s} \rightleftharpoons \text{Pt}_\text{s}\text{CO}_{2\text{s}}$	0.005	0	1×10^{13}	22
5	$\text{H}_2 + 2\text{Pt}_\text{s} \rightleftharpoons 2\text{Pt}_\text{s}\text{H}_\text{s}$	0.05	0	5×10^{12}	173
6	$\text{H}_2\text{O} + \text{Pt}_\text{s} \rightleftharpoons \text{Pt}_\text{s}\text{H}_2\text{O}_\text{s}$	0.1	0	1×10^{13}	45
7	$\text{Pt}_\text{s}\text{O}_\text{s} + \text{Pt} \rightleftharpoons \text{PtO}_{\text{ss}} + \text{Pt}_\text{s}$	3.3×10^8	0	1.9×10^{-2}	0
8	$\text{Pt}_\text{s}\text{C}_\text{s} + \text{Pt}_\text{s}\text{O}_\text{s} \rightleftharpoons \text{Pt}_\text{s}\text{CO}_\text{s} + \text{Pt}_\text{s}$	1×10^{13}	63	–	–
9	$\text{Pt}_\text{s}\text{H}_\text{s} + \text{Pt}_\text{s}\text{O}_\text{s} \rightleftharpoons \text{Pt}_\text{s}\text{OH}_\text{s} + \text{Pt}_\text{s}$	1×10^{13}	126	–	–
10	$\text{Pt}_\text{s}\text{CO}_\text{s} + \text{Pt}_\text{s}\text{O}_\text{s} \rightleftharpoons \text{Pt}_\text{s}\text{CO}_{2\text{s}} + \text{Pt}_\text{s}$	1×10^{13}	124	–	–
11	$2\text{Pt}_\text{s}\text{OH}_\text{s} \rightleftharpoons \text{Pt}_\text{s}\text{H}_2\text{O}_\text{s} + \text{Pt}_\text{s}\text{O}_\text{s}$	1×10^{13}	80	–	–
12	$\text{Pt}_\text{s}\text{OH}_\text{s} + \text{Pt}_\text{s}\text{H}_\text{s} \rightleftharpoons \text{Pt}_\text{s}\text{H}_2\text{O}_\text{s} + \text{Pt}_\text{s}$	1×10^{13}	106	–	–

from 25% and 23% at 800 °C to 53% and 45% at 950 °C, respectively. The responses have been modeled based on the reaction scheme presented in Table 1. Details of modeling TAP responses can be found in references [28,44,45]. Just like the reaction scheme used by de Smet et al. one single site was taken into account and the surface reactions have been assumed irreversible. The main difference to the scheme presented in Table 2 and those in the literature [46,47] is the inclusion of a step that accounts for sub-surface oxygen (step 7).

The sticking coefficients for the adsorption of CH_4 , O_2 and CO as well as the activation energies for CH_4 , O_2 and H_2 have been adjusted to fit the model with the experimental data. Rather high values of the activation energies for methane activation and hydrogen desorption have been estimated. A value of 75 kJ/mol is reported in the literature for H_2 desorption from reduced Pt. In this case hydrogen desorbs from Pt containing sub-surface oxygen thus a much stronger interaction might be expected. Unfortunately, de Smet et al. [35,36] did not observe the formation of hydrogen in their reactor and thus did not estimate a desorption energy for hydrogen. Otherwise the results of the two different approaches are rather consistent. Both studies indicated that an oxidized surface is necessary to activate methane and that CO is a primary reaction product. The reaction schemes are very similar and only a difference in the methane activation energy is observed.

Thus the intrinsic kinetics of fast reactions can be assessed by performing experiments with well-defined hydrodynamics and by taking explicitly the mass and heat transfer phenomena into account.

5. Perspectives and conclusions

The chemical reaction engineering approach consists of a computational model capable of predicting reactor performance based on the fundamental molecular-scale parameters describing the chemical kinetics and the transport coefficients. The chemical kinetics is measured experimentally in dedicated laboratory reactors. A rate equation corresponding to a reaction scheme based on elementary reaction steps is derived to describe the experimental data. The parameters in the rate equation are estimated by regression analysis. The rate expression thus based on the *intrinsic* reaction kinetics is incorporated into a reactor model to predict the behavior of the plant-scale reactor.

The good practice of kinetic experiments was discussed in the first part of this paper. More and more often kinetic models are based on a microkinetic approach [48–50]. This consists of a sequence of elementary steps without any assumption on the rate-determining step. The corresponding rate is usually calculated numerically. Microkinetics require forward and backward rate

parameters for each reaction step. These are usually obtained from independent experiments such as surface science or temperature-programmed experiments, or from computational chemistry. Some key parameters, identified by a sensitivity analysis, can then be adjusted by comparing the model to the experimental data. Once the parameters are fixed the rate-determining step can be found numerically by applying Campbell's "degree of rate control" [51]. Similar as the microkinetic modeling is the single event method, initially developed for complex networks involving reactions of hydrocarbons [52,53]. These methods give detailed insights into the reaction mechanism and can be very helpful in catalyst development. As no rate-determining step is assumed, these models will be more robust over a larger range of operating conditions and it will better predict the reaction dynamics. Coupled with a reactor model it should allow the simulation of start-up and shutdown of industrial reactors.

The second essential element in reactor modeling and scale-up consists of a detailed description of the transport phenomena for the industrial reactor and its operating conditions. This "computer-assisted" scale-up approach results in faster process development at lower cost by better planning the need for pilot-scale experiments or by completely avoiding these tests and by better reactor design.

Industrial reactors are nearly always operated in a regime where mass or energy transport affects the product distribution. Thus an understanding of the coupling between transport processes and chemical reactions is essential for the design and scale-up of an industrial reactor. In the last decades computational fluid dynamics has become an important tool in the field of chemical engineering and can allow for the understanding of the coupling between transport processes and chemical reactions. CFD models solve for the spatial distributions of the velocity, concentration, and temperature fields.

Only in the case of laminar flow, the models have a fundamental basis that involves molecular-scale transport coefficients. Laminar flow CVD reactors involving complex kinetics have been modeled by CFD approaches [54].

Most industrial reactors operate, however, in the turbulent flow regime. The randomness of packed-beds adds up to the complexity. Currently CFD of turbulent flow in packed-beds is in an initial development stage but very interesting insights are being reported [7]. These CFD models still contain some phenomenological parameters and experimental validation is indispensable. Recently developed experimental techniques, such noninvasive tomographic methods [55] and magnetic resonance imaging (MRI) [56] are currently being employed to obtain local velocity fields.

Each of these techniques have its own limitations [7], but coupled with detailed CFD calculations it can provide a very

powerful combination to obtain fundamental insights in mass and heat transport in complex geometries such as packed-beds.

References

- [1] K. Wintermantel, *Chem. Eng. Sci.* 54 (1999) 1601.
- [2] J.J. Lerou, K.M. Ng, *Chem. Eng. Sci.* 51 (1996) 1595.
- [3] D. Majumder, L.J. Broadbelt, *AIChE J.* 52 (2006) 4214–4228.
- [4] R.J. Berger, E.H. Stitt, G.B. Marin, F. Kapteijn, J.A. Moulijn, *Cattech* 5 (2001) 30.
- [5] M. Neurock, S.A. Wasileski, D. Mei, *Chem. Eng. Sci.* 59 (2004) 4703.
- [6] R.A. van Santen, X. Rozanska, *Adv. Chem. Eng.* 28 (2001) 399.
- [7] A.G. Dixon, M. Nijemeisland, E.H. Stitt, *Adv. Chem. Eng.* 31 (2006) 307.
- [8] G.F. Froment, K. Bischoff, *Chemical Reactor Analysis and Design*, second ed., John Wiley and Sons, New York, 1990.
- [9] D. Schweich (Ed.), *Génie de la réaction chimique*, TEC & DOC, 2001.
- [10] A. Dybbs, R.V. Edwards, in: J. Bear, M. Corapcioglu (Eds.), *Fundamentals of Transport Phenomena in Porous Media*, Martinus Nijhoff, Dordrecht, 1984, p. 201.
- [11] F. Kapteijn, J.A. Moulijn, in: G. Ertl, H. Knözinger, J. Weitkamp (Eds.), *Handbook of Heterogeneous Catalysis*, vol. 3, VCH, Weinheim, 1997, pp. 1359–1376.
- [12] D.E. Mears, *Ind. Eng. Chem. Process Des. Dev.* 10 (1971) 541.
- [13] C.N. Satterfield, *Mass Transfer in Heterogeneous Catalysis*, MIT Press, Cambridge, 1970.
- [14] J.M. Commenge, L. Kalk, J.P. Corriou, M. Matlosz, *Microchannel reactors for kinetic measurement: influence of diffusion and dispersion on experimental accuracy.*, in: *IMRET 5: Proceedings of the fifth international conference on microreaction technology*, 2001, pp. 131–140.
- [15] R.J. Berger, F. Kapteijn, *Ind. Eng. Chem. Res.* (2006) 3863–3870.
- [16] G. Germani, P. Alphonse, M. Courty, Y. Schuurman, C. Mirodatos, *Catal. Today* 110 (2005) 114–120.
- [17] G. Germani, Y. Schuurman, *AIChE J.* 52 (2006) 1806–1813.
- [18] X. Ouyang, L. Bednarova, R.S. Besser, P. Ho, *AIChE J.* 51 (2005) 1758–1772.
- [19] E.V. Rebrov, G.B.F. Seijger, H.P.A. Calis, M.H.J.M. de Croon, C.M. van den Bleek, J.C. Schouten, *Appl. Catal. A: Gen.* 206 (2001) 125–143.
- [20] N. Dupont, G. Germani, A.C. van Veen, Y. Schuurman, G. Schäfer, C. Mirodatos, *Int. J. Hydrogen Energy* 32 (2007) 1443–1449.
- [21] G. Groppi, W. Ibashi, E. Tronconi, P. Forzatti, *Chem. Eng. J.* 82 (2001) 57–71.
- [22] I. Tavazzi, A. Beretta, G. Groppi, P. Forzatti, *J. Catal.* 241 (2006) 1–13.
- [23] H. Redlingshöfer, A. Fischer, C. Weckbecker, K. Huthmacher, G. Emig, *Ind. Eng. Chem. Res.* 42 (2003) 5482–5488.
- [24] M. Maestri, A. Beretta, G. Groppi, E. Tronconi, P. Forzatti, *Catal. Today* 105 (2005) 709.
- [25] L. Kiwi-Minsker, I. Yuranov, V. Höller, A. Renken, *Chem. Eng. Sci.* 54 (1999) 4785.
- [26] I. Yuranov, L. Kiwi-Minsker, A. Renken, *Appl. Catal. B: Environ.* 43 (2003) 217.
- [27] J.T. Gleaves, G.S. Yablonskii, P. Panawadee, Y. Schuurman, *Appl. Catal. A: Gen.* 160 (1) (1997) 55.
- [28] Y. Schuurman, *Catal. Today* 121 (2007) 187–196.
- [29] O.V. Buyevskaya, K. Walter, D. Wolf, M. Baerns, *Catal. Lett.* 38 (1996) 81.
- [30] E.P.J. Mallens, J.H.B.J. Hoebink, G.B. Marin, *J. Catal.* 167 (1997) 43.
- [31] M. Fahti, F. Monnet, Y. Schuurman, A. Holmen, C. Mirodatos, *J. Catal.* 190 (2000) 439–445.
- [32] Y. Schuurman, C. Marquez-Alvarez, V.C.H. Kroll, C. Mirodatos, *Catal. Today* 46 (1998) 207–214.
- [33] J. Pérez-Ramírez, E.V. Kondratenko, V.A. Kondratenko, M. Baerns, *J. Catal.* 227 (1) (2004) 90–100.
- [34] S. Delagrangé, Y. Schuurman, *Catal. Today* 121 (2007) 204–209.
- [35] C.R.H. de Smet, M.H.J.M. de Croon, R.J. Berger, G.B. Marin, J.C. Schouten, *Appl. Catal. A: Gen.* 187 (1999) 33–48.
- [36] C.R.H. de Smet, M.H.J.M. de Croon, R.J. Berger, G.B. Marin, J.C. Schouten, *AIChE J.* 46 (9) (2000) 1837.
- [37] J.R. Rostrup-Nielsen, *Catal. Today* 18 (1993) 305.
- [38] D.A. Hickman, L.D. Schmidt, *J. Catal.* 138 (1992) 267.
- [39] O. Deutschmann, L.D. Schmidt, *AIChE J.* 44 (1998) 2465.
- [40] F. Monnet, Y. Schuurman, F. Cadete Santos Aires, J.C. Bertolini, C. Mirodatos, *Catal. Today* 64 (2001) 51–58.
- [41] F. Monnet, Y. Schuurman, F.J. Cadete Santos Aires, J.C. Bertolini, C. Mirodatos, *C. R. Acad. Sci. Paris, Serie IIC, Chimie/Chem.* 3 (2000) 577–581.
- [42] E.P.J. Mallens, J.H.B.J. Hoebink, G.B. Marin, *Catal. Lett.* 33 (1995) 291.
- [43] S.W. Churchill, M. Bernstein, *J. Heat Trans.* 99 (1977) 301.
- [44] S.C. Van der Linde, T.A. Nijhuis, F.H.M. Dekker, F. Kapteijn, J.A. Moulijn, *Appl. Catal. A: Gen.* 151 (1997) 27.
- [45] M. Soick, D. Wolf, M. Baerns, *Chem. Eng. Sci.* 55 (2000) 2875.
- [46] D.A. Hickman, L.D. Schmidt, *AIChE J.* 39 (1993) 1164.
- [47] O. Deutschmann, F. Behrendt, J. Warnatz, *Catal. Today* 21 (1994) 461.
- [48] J.A. Dumesic, D.F. Rudd, L.M. Aparicio, J.E. Rekoske, A.A. Trevino, *The Microkinetics of Heterogeneous Catalysis*, American Chemical Society, Washington, DC, 1993.
- [49] L.J. Broadbelt, R.Q. Snurr, *Appl. Catal. A: Gen.* 200 (2000) 23–46.
- [50] P. Stoltze, *Prog. Surf. Sci.* 65 (2000) 65–150.
- [51] C.T. Campbell, *Top. Catal.* 1 (1994) 353.
- [52] G.F. Froment, *Catal. Rev.* 47 (2005) 83–124.
- [53] P. Galtier, *Adv. Chem. Eng.* 32 (2007) 259.
- [54] K.J. Kuijlaars, C.R. Kleijn, H.E.A. Van den Akker, *Mater. Sci. Semicond. Process.* 1 (1) (1998) 43–54.
- [55] J. Chaouki, F. Larachi, M.P. Dudukovic, *Ind. Eng. Chem. Res.* 36 (1997) 4476–4503.
- [56] L.F. Gladden, M.D. Mantle, A.J. Sederman, *Adv. Catal.* 50 (2006) 1–75.